Marine Geology 230 (2006) 161 – 177

MARINE GEOLOGY
INTERNATIONAL JOURNAL OF MARINE GEOLOGY, GEOCHEMISTRY AND GEOPHYSICS

www.elsevier.com/locate/margeo

Geochemical and stratigraphic indicators of late Holocene coastal evolution in the Gythio area, southern Peloponnese, Greece

A.B. Cundy [a,*], D. Sprague [a], L. Hopkinson [b], H. Maroukian [c], K. Gaki-Papanastassiou [c], D. Papanastassiou [d], M.R. Frogley [a]

[a] *Centre for Environmental Research, University of Sussex, Brighton, BN1 9QJ, UK*
[b] *School of the Environment, University of Brighton, Brighton, BN2 4GJ, UK*
[c] *Department of Geography-Climatology, University of Athens, Gr 15784 Athens, Greece*
[d] *Institute of Geodynamics, National Observatory of Athens, Gr 11810 Athens, Greece*

Received 5 October 2005; received in revised form 20 March 2006; accepted 9 April 2006

Abstract

The study of past changes in sea level, and of historical and pre-historical coastal evolution, using coastal sediment stratigraphies is well-established over a range of geographic areas, in both seismic and aseismic settings. In the eastern Mediterranean, however, such studies are less common, and, notably, the use of sediment geochemistry, and its combination with lithostratigraphic studies to analyze palaeoenvironmental and palaeo-sea-level change, has not been explored to any significant extent, despite the fact that geochemical data have been successfully used elsewhere to aid in the identification of sea-level changes. Here, we use a combined geochemical, stratigraphic and microfossil approach to reconstruct late Holocene coastal evolution and sea-level change at two sites near Gythio in the southern Peloponnese, Greece. The sites show stratigraphic and geochemical evidence of the presence in Late Helladic times (ca. 1500 BC) of barrier-protected coastal lagoonal/wetland environments, which have gradually infilled over the last ca. 3500 yr. Archaeological remains and ceramic and charcoal-bearing horizons within the sediment sequences indicate Late Roman occupation of the area, although there is no sedimentary evidence of significant pre-Roman activity at the study sites. An apparent brackish wetland peat deposit at −3.4 m (overlain by anoxic lagoonal clays) at Kamares (Kato Vathi) Bay shows a calibrated radiocarbon age of 1640–1440 BC, suggesting a relative sea-level rise of 0.8–1 mm/yr in this area over the past 3500 yr, in good agreement with previous archaeological and sea-level modelling studies. There is no evidence, based on the stratigraphic, microfossil or geochemical record, of sudden marine flooding events related to local or regional seismic activity, despite the presence of the area in a seismically active zone known to be subject to periodic earthquakes and tsunami. The data highlight the utility of combining geochemical and stratigraphic studies in the reconstruction of coastal evolution and the study of palaeo-sea-level changes, particularly in sequences (such as those described here) where microfossils are poorly preserved.

Keywords: sea level; coastal geomorphology; coastal sediments; geochemistry; Greece; Eastern Mediterranean

1. Introduction

The study of past changes in sea level, and of historical and pre-historical coastal evolution, using coastal

* Corresponding author. Tel.: +44 1273 678737; fax: +44 1273 678937.
E-mail address: A.B.Cundy@sussex.ac.uk (A.B. Cundy).

0025-3227/$ - see front matter © 2006 Elsevier B.V. All rights reserved.
doi:10.1016/j.margeo.2006.04.009

sediment stratigraphies is relatively well-established over a range of geographic areas, in both seismically-active and aseismic settings (e.g. Long and Shennan, 1994; Devoy et al., 1996; Nelson et al., 1996; Islam and Tooley, 1999; Goff and Chague-Goff, 1999; Cundy et al., 2000, 2002; Hamilton and Shennan, 2005). Such studies typically use detailed lithological and palaeontological analysis of coastal sediment sequences to reconstruct past environmental conditions and changes in relative sea level, the latter often being recorded by distinct lithological changes between peaty soils and intertidal muds, and associated changes in microfossil assemblages (e.g. Long and Shennan, 1994). In the Eastern Mediterranean region, however, studies of sea-level change, and particularly recent (late Holocene) rapid sea-level changes associated with tectonic activity, have tended to focus on the analysis of displaced archaeological remains and former erosional or bioconstructional shoreline features (e.g. coastal notches, algal reefs, etc.) (e.g. Flemming and Webb, 1986; Laborel and Laborel-Deguen, 1994; Maroukian et al., 1994; Stiros et al., 2000; Kershaw et al., 2005; Pirazzoli, 2005; Gaki-Papanastassiou et al., 2006a). Studies using coastal sediment sequences have (until recently) been less common, particularly for the analysis of more recent sea-level change (Cundy, 2005). Notably, the use of sediment geochemistry, and its combination with lithostratigraphic studies to analyze palaeoenvironmental and palaeo-sea-level change, has not been explored to any significant extent, despite the fact that geochemical data have been successfully used elsewhere to aid in the identification of sea-level changes (Thomas and Varekamp, 1991; Goff and Chague-Goff, 1999; Chague-Goff et al., 2002). Here, we use a combined geochemical, stratigraphic and microfossil approach to reconstruct late Holocene coastal evolution and sea-level change at two sites in the Gythio area, southern Peloponnese, Greece. Results obtained are compared with archaeological

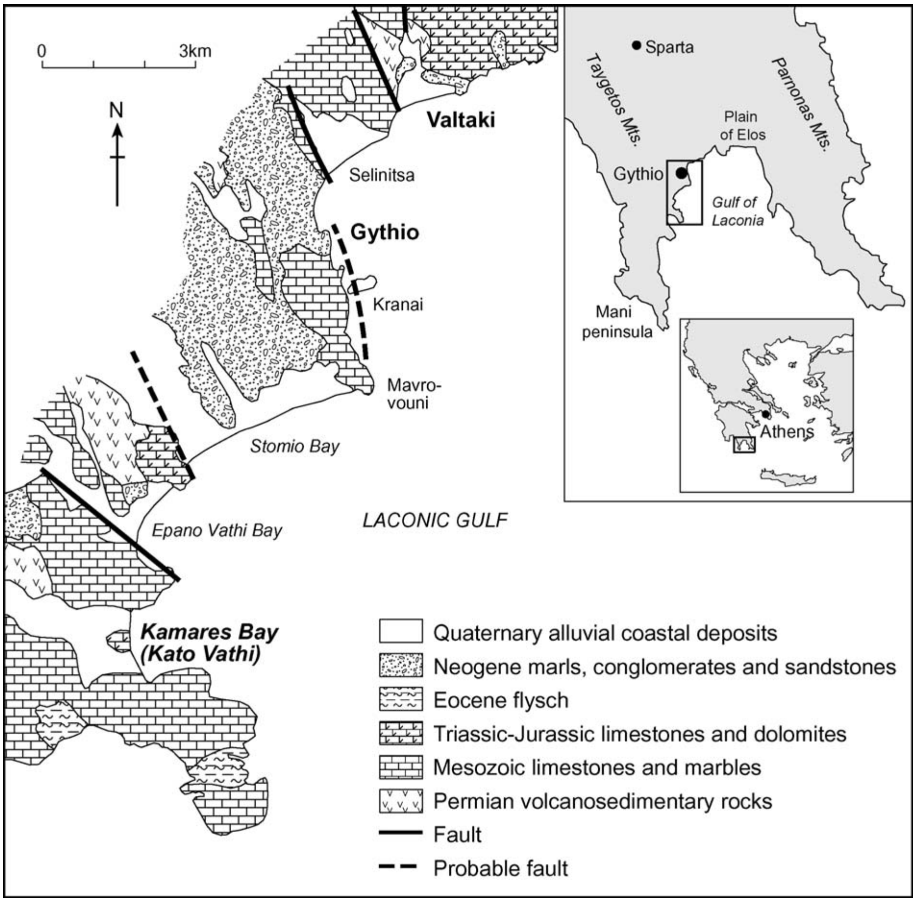

Fig. 1. General geological and geomorphological setting of the northeast coast of the Mani peninsula, S. Peloponnese, Greece (after Gaki-Papanastassiou et al., 2006b).

evidence and with published local relative sea-level curves and earthquake/tsunami records. More widely, the general applicability, and limitations, of using bulk geochemical data to examine coastal palaeoenvironmental and palaeo-sea-level change are evaluated.

2. Regional setting/study area

The two study areas (Kamares (Kato Vathi) and Valtaki Bay) are located on the northeast coast of the Mani peninsula, southern Peloponnese, Greece, adjacent to the Gulf of Laconia (Fig. 1). Morphotectonically, the Laconic Gulf (and its northern extension) form an asymmetric graben between the mountain masses of Parnonas (1935 m) in the east and Taygetos (2407 m) in the west. The area is characterised by intense seismicity: strong earthquakes (from local and regional tectonic activity) have affected the area in 365 AD, 1750 AD, 1795/1798 AD, 1842 AD, 1866 AD, 1867 AD, 1927 AD and 1944 AD, with tsunami reported for the 365 AD, 1866 AD, and 1867 AD events (Papazachos and Papazachou, 1997). The region has a relatively long history of human activity (archaeological remains are present from the Middle Palaeolithic period, Panagopoulou et al., 2002), with the

(a)

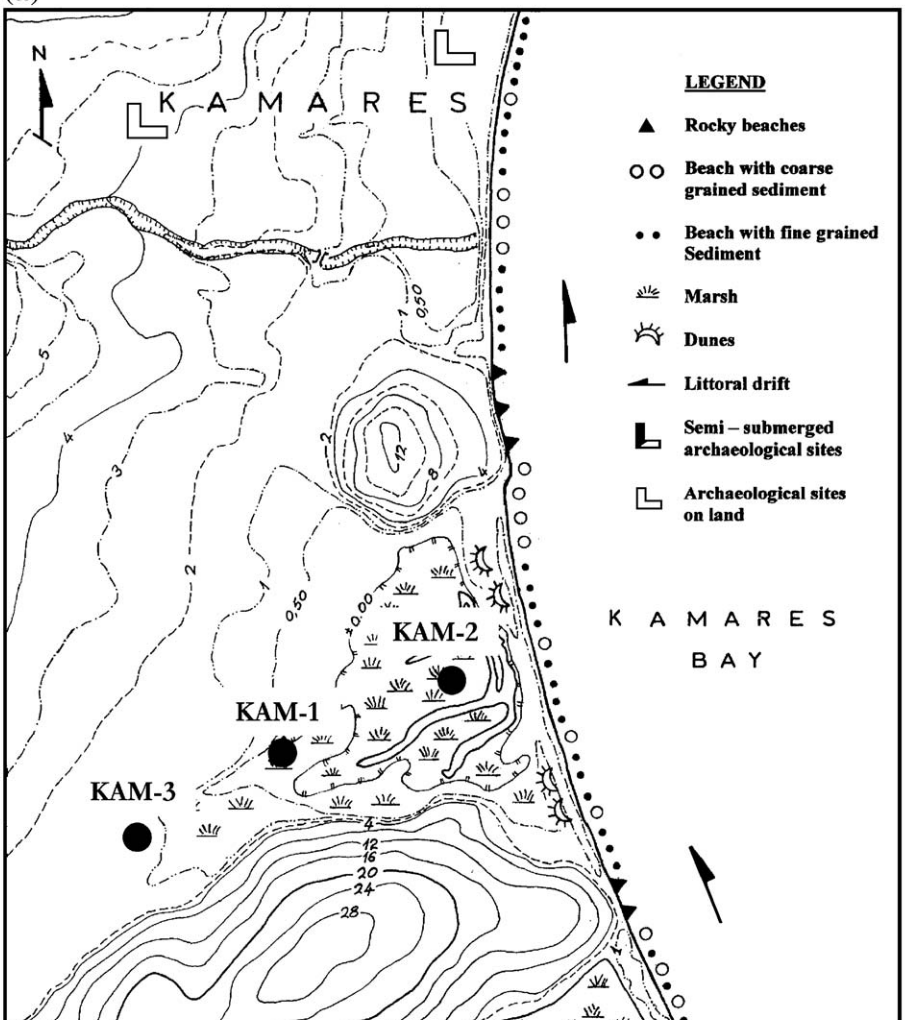

Fig. 2. Study sites: (a) Kamares (Kato Vathi) Bay and (b) Valtaki Bay, near Gythio, S. Peloponnese, Greece. Coring locations are marked with black circles. Contours and spot heights show elevation in metres.

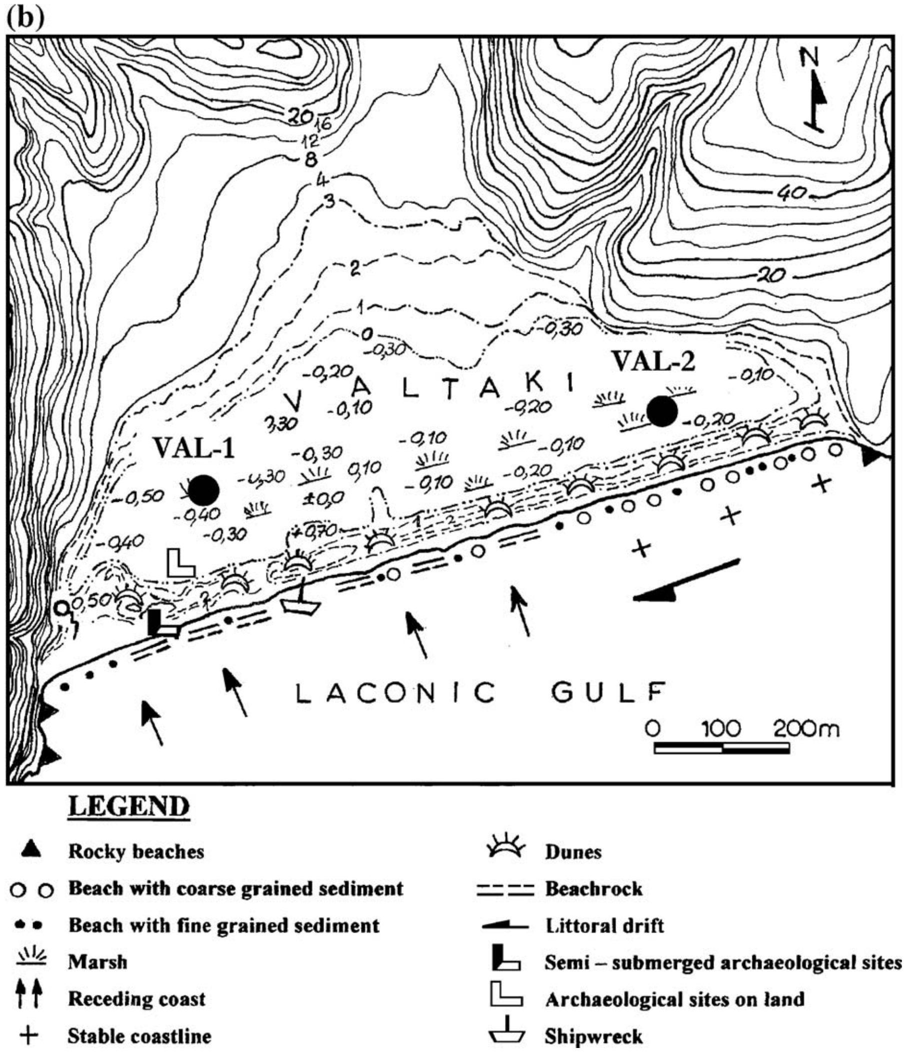

Fig. 2 (*continued*).

Elos plain at the north of the Gulf being the proposed location of the Mycenean settlement of Elos (a tributary port to Sparta and Mycenae, referred to in Homer's Iliad) (Kraft et al., 1977). In addition, Late Roman/Early Byzantine archaeological remains are relatively common in the area (Gaki-Papanastassiou et al., 2006b). Gythio itself was an important port of Sparta during Classical and Hellenistic times (5th–2nd century BC), and became a significant Roman centre after 195 BC.

The general morphology of the coastal area studied is controlled by a series of en echelon normal faults which trend NW–SE and dip to the NE, producing a series of limestone promontories and low-lying, barrier-protected pocket embayments (Fig. 1). Kamares (Kato Vathi) Bay is located approximately 10 km south of Gythio, and consists of two low-lying coastal plain areas between (Middle Triassic to Upper Jurassic) limestone promontories. Permian to Lower Triassic schists and phyllites are also locally present. The site studied here consists of a small ephemeral lagoon/salt marsh (grading into poor quality pastoral farmland), situated behind a 1–2 m high sand and shingle barrier (Fig. 2a).

Valtaki Bay (Fig. 2b) is located approximately 5 km north of Gythio, and consists of a Holocene alluvial plain backed by Upper Cretaceous to Eocene limestones, Middle to Upper Triassic dolomites, Neogene marine clays and marls and Permian basic to intermediate tuffs and tufites. The plain is mostly cultivated, although ephemeral marshes are present in lower-lying areas immediately behind the coastal dunes. Quaternary alluvial deposits are present at the rear of the plain. The modern-day shoreline is fronted by a beach barrier (ca.

3–4 m high) of beach sands and vegetated dunes. Beach rock occurs locally in the subtidal beach face, and submerged Late Roman–Early Byzantine walls are present at the southwestern part of the beach barrier (Fig. 2b). These walls continue into the dune system, where they have been buried by dune sand deposits. A prominent fault scarp is present at the southwestern end of the bay, although there is no recorded evidence of historical earthquake activity on this fault (Papazachos and Papazachou, 1997).

3. Materials and methods

Stratigraphic data were collected at each site in September 2004 using an Atlas vibratory corer. Three 4-m-long cores (KAM1–KAM3) were collected from the Kamares Bay site (Fig. 2a) and two >2.5-m-long cores (VAL1 and VAL2) were collected at the Valtaki site (Fig. 2b). Core elevations were determined using a Jena 020A theodolite unit. In the absence of a reliable elevation benchmark, core elevations were initially determined relative to temporary benchmarks, and then surveyed to contemporary sea level. All elevations are therefore reported relative to contemporary sea level on 25th September 2004. The mean tidal range in the area is 4 cm (based on the Gythio tide gauge). Cores were described and logged, and then sub-divided in the field. All core sub-samples were refrigerated (at 4 °C) prior to analysis.

To determine recent sediment accumulation rates at each site, selected near-surface sub-samples were counted for at least 8 h on a Canberra well-type ultra-low background HPGe gamma ray spectrometer to determine the activities of ^{137}Cs, ^{210}Pb and other gamma emitting radionuclides. Spectra were analyzed using the Genie 2000 system and accumulated using a 16K channel integrated multichannel analyzer. Energy and efficiency calibrations were carried out using bentonite clay spiked with a mixed gamma-emitting radionuclide standard, QCYK8163, and checked against IAEA certified reference materials (e.g. IAEA 135). Detection limits were ca. 3 Bq/kg. Two sub-samples from 65–70 cm depth and 445–455 cm depth in the most landward Kamares Bay, core KAM3 (consisting of large charcoal fragments and a prominent peat unit respectively), were ^{14}C-dated via accelerator mass spectrometry (at the Beta Analytic Radiocarbon Dating Laboratory, Florida, USA) to provide further chronological control.

Samples were examined under an optical (reflected light) microscope at 40–80× magnification for microfossil (foraminifera and ostracod) content, following disaggregation with 5% H_2O_2 and separation of the >63 μm grain size fraction (Griffiths and Holmes, 2000; Gehrels, 2002). Bulk samples were also scanned for the presence of diatoms and other microflora using a Leo S420 Scanning Electron Microscope.

All samples were analyzed using a Panalytical Minipal 2 energy-dispersive X-ray fluorescence spectrometer (with 30 kV Rh-tube) to obtain compositional data. Samples were oven-dried, any large (>1 cm) pebbles removed, and the remaining sample ground to a fine powder using a ball mill and pelletised for trace and major element determinations. Accuracy was assessed by comparing a range of reference sample determinations (e.g. GSS-1) with recommended values. Precision and detection limits are element dependent; for the elements examined here precision (1σ) is better than 4 ppm (trace elements) and 0.6 wt.% (major elements) over the range of sample concentrations encountered, while detection limits are typically < 10 ppm (trace elements) and < 0.1 wt.% (major elements). Selected samples were also analyzed using a Leo S420 Scanning Electron microscope with an Inca 200 X-ray detection unit.

4. Results

4.1. Stratigraphic studies

4.1.1. Kamares Bay

The stratigraphy in the two landward cores in the Kamares Bay transect (KAM-1 and KAM-3) is dominated by silt and clay units (Fig. 3a). The basal units of these cores (2.9–3.5 m below contemporary sea level (bsl)) consist of dark grey/black, malodorous, interbedded clays and peats, although there is a sharp (erosional?) contact at the base of core KAM-1 into a unit of grey clay with coarse sand. Prominent peat units occur in KAM-1 at 295–306 cm bsl, and KAM-3 at 354–329 cm bsl and 316–306 cm bsl. Above ca. 2.9 m bsl, organic material is much less common, being found dominantly as dispersed root material, with occasional woody fragments. In addition, in both cores the dark grey/black clays grade into silty clay units above 2.9 m bsl which are much lighter in colour, and show distinct orange-brown mottling. Angular limestone clasts (0.5–2 cm diameter) commonly occur in these lighter coloured silty clay units. Occasional brick/tile fragments are present at 182 cm bsl in KAM-3. Sand units are present at 38 cm bsl in core KAM-1 (consisting of a 2 cm thick unit of compact fine sand), and at 64–80 cm bsl (medium to coarse sand) and 35–64 cm bsl (coarse sand and grit with silt) in KAM-3. These sand units are apparently localised and cannot be traced between cores. Notably, a prominent unit of orange-brown silty clay, containing burnt (i.e. reddened) brick and tile fragments

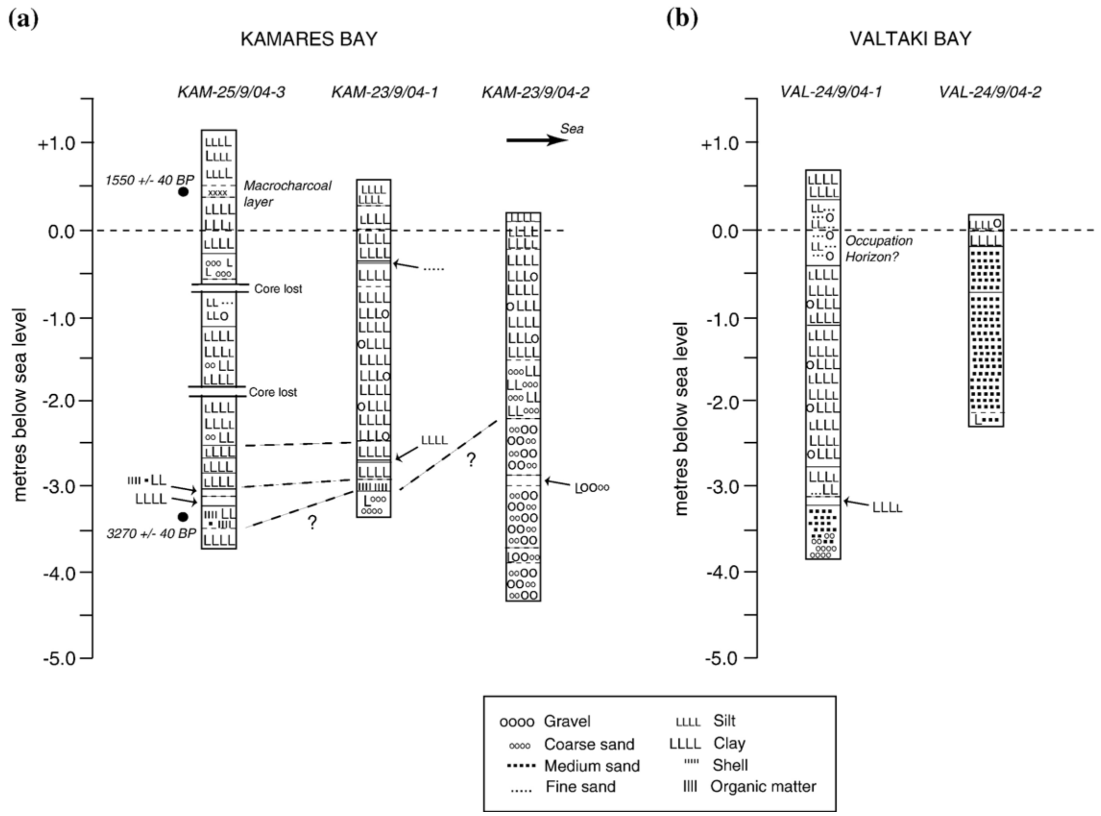

Fig. 3. Simplified diagram of the coastal stratigraphy for (a) Kamares Bay, (b) Valtaki Bay. See Fig. 2 for core locations. All core elevations are relative to contemporary sea level on 25th September 2004.

and large (>5 mm) pieces of charcoal, was present at 38–47 cm above contemporary sea level (asl) in core KAM-3. This grades upwards into a massive, compact, light brown clayey-silt with common root material, which is also found at sites KAM-1 and 2, and forms the present-day soil. No obvious shell material was observed in any of the three cores in the transect.

Core KAM-2, the most seaward of the three cores (80 m behind the present beach barrier) shows a deeper stratigraphy (i.e. 225–435 cm bsl) dominated by coarse sand and semi-rounded grit and gravel deposits. The grits consist of quartz and metabasic/schistose clasts, and are similar in shape and composition to the present-day beach barrier material. At 225 cm bsl these coarser deposits grade into a coarse sand and clay unit, with occasional angular clasts (diameter ca. 5–10 mm) and common root fragments. This in turn grades at 154 cm bsl into a grey clay with some orange-brown mottling, with angular clasts and occasional root fragments. At 25 cm bsl a light brown silty-clay unit with occasional root matter is present, which grades into light brown friable silt containing occasional root matter at 6 cm asl. This unit continues to the ground surface.

4.1.2. Valtaki Bay

Due to the presence of extensive dune deposits at Valtaki, and widespread colluvial wedges at the rear of the site, coring was limited to two sites (VAL-1 and VAL-2), approximately 100 m and 150 m from the shoreline respectively (Fig. 2b). Core VAL-1, collected from the southwest of the site, contains a basal unit (390–331 cm bsl) of orange-brown coarse to medium sand which fines upwards, which is overlain by an orange-brown silty clay, grading into (at 320 cm bsl) a grey-black silty-clay unit with occasional sand (Fig. 3b). This is in turn overlain by grey-brown medium sand, and at 284 cm bsl a prominent unit of grey-black silty clay. This unit contains occasional sub-angular limestone and rounded mafic volcanic clasts (diameter ca. 5–15 mm), root fragments and finely dispersed organic material. At 118 cm bsl this unit becomes grey in colour, but otherwise is similar to that below. Root material ceases to be present above 88 cm bsl, although above 63 cm bsl isolated brick/tile fragments are found. At 45 cm bsl a prominent unit of mottled, grey silty-sand is present, which contains numerous brick/tile fragments (up to 2 cm diameter), woody root and stem fragments, and large angular (possibly artificially cut) clasts (diameter ca. 40 mm) of porphyritic volcanic rock. The common presence of brick/tile fragments, and possibly worked fragments of (exotic) porphyry (an ornamental stone) indicates that this layer is an occupation horizon. While the brick/tile fragments are not archaeologically diagnostic, they are identical in appearance to those in the Late Roman archaeological remains found in the area of the contemporary beach, indicating a Late Roman age. Clasts become smaller above 12 cm asl, until at 25 cm asl a sharp contact is made with a dark brown-grey silty-clay unit containing woody material and plant roots, which extends to the present-day soil surface.

In contrast, the stratigraphy of core VAL-2 (Fig. 3b) is dominated by a massive medium sand unit, which extends from 227 to 16 cm bsl. This is overlain by grey clay showing some orange mottling and occasional root material, which grades into light brown silt at approximately contemporary sea level. This unit is rich in root material, and continues to the soil surface.

4.2. Radiometric dating

In order to examine recent (i.e. within the past 120 yr) sediment accumulation processes at each site, near-surface sediments were dated using the ^{210}Pb method. ^{137}Cs was also determined to corroborate (or otherwise) the ^{210}Pb data. ^{210}Pb (half-life = 22.3 yr) is a naturally-produced radionuclide that has been extensively used in the dating of recent sediments. Dating is based on determination of the vertical distribution of ^{210}Pb derived from atmospheric fallout (termed unsupported ^{210}Pb, or $^{210}Pb_{excess}$), and the known decay rate of ^{210}Pb (see Appleby and Oldfield, 1992 for further details of the ^{210}Pb method). Normally, the ^{210}Pb dating method is limited to sedimentary deposits less than 120–150 yr old (i.e. 5–7 half-lives of ^{210}Pb), which is typically taken as the period over which $^{210}Pb_{excess}$ decays

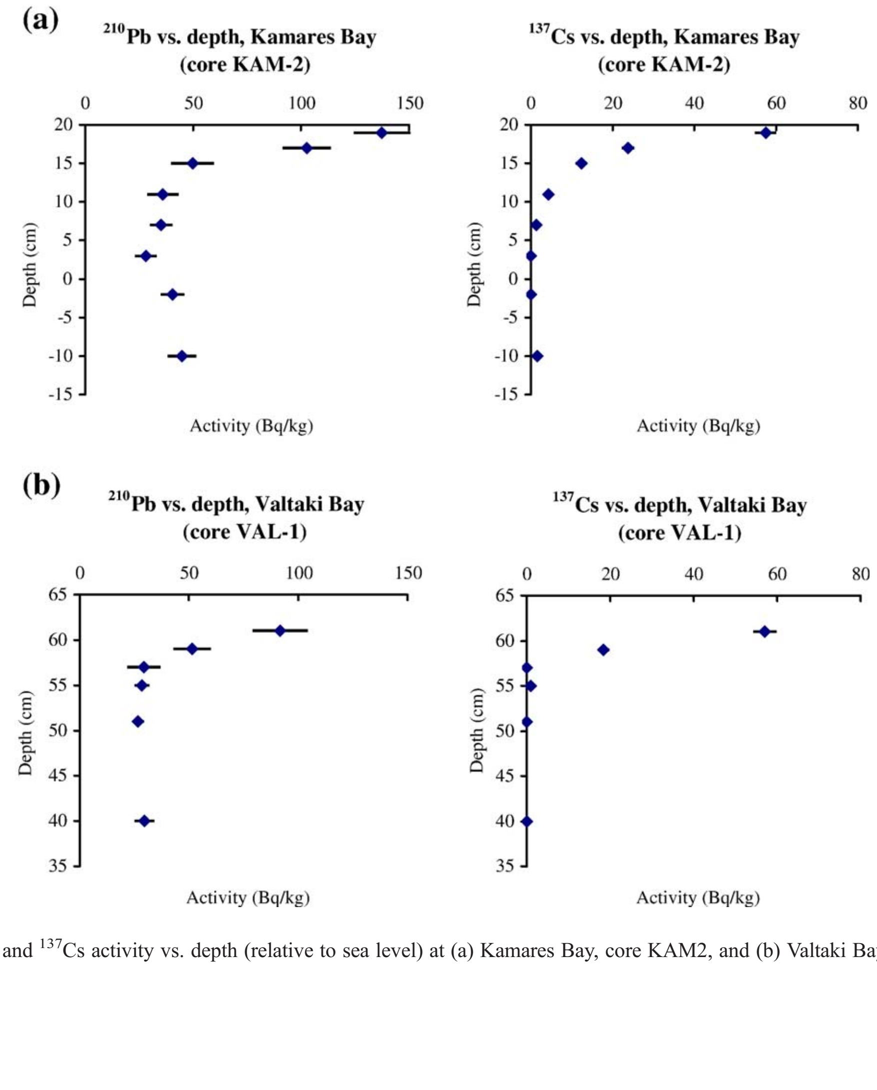

Fig. 4. ^{210}Pb and ^{137}Cs activity vs. depth (relative to sea level) at (a) Kamares Bay, core KAM2, and (b) Valtaki Bay, core VAL1.

to negligible or unmeasurable activities. ^{137}Cs (half-life = 30 yr) is an artificially produced radionuclide, introduced to the study area by atmospheric fallout from nuclear weapons testing and nuclear reactor accidents. Global dispersion of ^{137}Cs began in 1954 AD, with marked maxima in the deposition of ^{137}Cs occurring in the northern hemisphere in 1958 AD, 1963 AD (from nuclear weapons testing) and 1986 AD (from the Chernobyl accident). In favourable conditions, periods of peak fallout/discharge provide subsurface activity maxima in accumulating sediments which can be used to derive rates of sediment accumulation (e.g. Ritchie et al., 1990; Cundy and Croudace, 1996). Notably, the distributions of both ^{210}Pb and ^{137}Cs can be used to indicate recent changes in sedimentation due to events such as barrier overwash (e.g. Cundy et al., 2003). Consequently, ^{210}Pb and ^{137}Cs assay focussed on those cores nearest to the contemporary coastal barrier (KAM-2 and VAL-1) and located in ephemeral wetland areas which were less likely to have been disturbed by recent agricultural activity. At both the Kamares Bay and Valtaki Bay sites, ^{210}Pb and ^{137}Cs show an approximately exponential decline with depth, with maximum activities occurring at the present-day soil surface (Fig. 4). At Kamares Bay, ^{137}Cs falls to undetectable activities at 10 cm asl (i.e. 10 cm below the contemporary soil surface), with ^{210}Pb declining to near-constant (i.e. supported) activities at the same depth. At Valtaki, ^{137}Cs declines to undetectable activities at 57 cm asl (i.e. 5 cm below the contemporary soil surface), and ^{210}Pb to constant (supported) activities at the same depth. The similarity between the ^{137}Cs and ^{210}Pb$_{excess}$ profiles at each site, the shallow depth over which both radionuclides are present at detectable activities, and the lack of any subsurface maxima in the ^{137}Cs profiles indicate that there has been little recent sediment accumulation at either site: the distributions of both ^{137}Cs and ^{210}Pb are consistent with limited bioturbative downcore mixing from a higher activity surface layer.

Two deeper samples from Kamares Bay were dated via ^{14}C assay (Table 1): a macro-charcoal sample from the charcoal- and ceramic-rich orange silty clay at 38–47 cm asl in KAM-3, and a peat sample from 334–344 cm bsl, also from KAM-3, in the dark grey/black interbedded clays and peats at the base of the cored sequence. The charcoal sample yielded a conventional radiocarbon age of 1540 ± 40 BP (calibrated age 420–600 AD; all radiocarbon ages were calibrated using the INTCAL04 database, following Reimer et al., 2004). The deeper peat sample yielded a conventional radiocarbon age of 3270 ± 40 BP (calibrated age 1640–1440 BC). This late Holocene age indicates that the entire cored sequence at Kamares Bay has been deposited since the relative stabilisation of sea level in the Mediterranean in the mid-Holocene (e.g. Lambeck, 1996). Based on the calibrated radiocarbon ages of these two samples, the average net sediment accumulation rate at Kamares Bay between ca. 1500 BC and 500 AD was ca. 2 mm/yr. Post-ca. 500 AD, this rate decreased to 0.4 mm/yr. It should be noted, however, that these average rates are likely to mask considerable variation in sediment accumulation/erosion rates, given the significant sedimentological variations observed in the KAM-3 core, and the sharp contacts between units (Fig. 3a) which indicate the occurrence of erosive episodes.

No samples from Valtaki were dated by ^{14}C, due to an absence of appreciable, in-situ, organic or carbonate material. If it is assumed that the proposed occupation horizon at 45 cm bsl in core VAL-1, however, is Late Roman in age (based on archaeological evidence—see Section 4.1.2), a net sediment accumulation rate of 0.2–0.6 mm/yr over the post-Roman period (ca. 400 AD to present) is indicated, similar to that observed at Kamares Bay.

4.3. Microfossils

Despite core samples being examined for ostracods, foraminifera and diatoms via detailed optical and scanning electron microscope study, no intact fossil remains were detected, apart from isolated beetle remains and comminuted shell fragments at the surface of core VAL-1. The absence of identifiable carbonate microfossils is probably related to poor preservation (dissolution), as cores from both sites record low concentrations of

Table 1
Radiocarbon dates from sedimentary material from core KAM-3, Kamares Bay site

Sample depth (cm above (asl) or below (bsl) sea level)	Material dated	Conventional ^{14}C age (^{14}C yr BP ± 1σ)	Calibrated age (2σ range)	^{13}C/^{12}C ratio (‰)	Laboratory reference
38–47 cm asl	Charcoal	1550 ± 40	AD 420–600	−24.5	Beta—201656 (AMS)
334–344 cm bsl	Peat	3270 ± 40	BC 1640–1440	−26.8	Beta—201657 (AMS)

Radiocarbon age calibrations were performed using the INTCAL04 database (Reimer et al., 2004), using the programme CALIB 5.0 (Stuiver and Reimer, 1993).

carbonate (see Section 4.5) despite the local limestone-rich geology. In the basal (>3 m bsl) organic-rich units in cores KAM-3 and KAM-1, SEM examination showed the presence of large (ca. 50–100 μm) fragments of relatively well-preserved stem and root material, with common pyrite framboids (Fig. 5), but no evidence of diatom flora. It is not clear whether the absence of diatoms in these highly productive, organic-rich units is due to low initial concentrations of these organisms, or diagenetic dissolution.

4.4. Stable carbon isotope data

A number of authors have used δ^{13}C values as indicators of palaeovegetation change, and notably in coastal environments as indicators of palaeosalinity, due to an increased dominance of C-4 plants as salinity increases (e.g. DeLaune, 1986; Chmura and Aharon, 1995; Mackie et al., 2005; Wilson et al., 2005). δ^{13}C values determined as part of the standard AMS ^{14}C assay on the two radiocarbon-dated samples from core KAM-3, at 38–47 cm asl and 334–344 cm bsl, are relatively ^{13}C-depleted (Table 1), at −24.5‰ and −26.8‰ respectively. The δ^{13}C value for the former (macro-charcoal) sample is consistent with its derivation from burnt wood fragments. The δ^{13}C value for the peat at 334–344 cm bsl is highly ^{13}C-depleted. The organic matter in this peat layer is relatively well-preserved (Fig. 5), possibly due to the sulphidic nature of the sediments here (see Section 4.5), indicating that this δ^{13}C-depleted value is not a consequence of significant negative shifts caused by intense decomposition of organic matter, but instead reflects the δ^{13}C value in the original vegetation (see Chmura and Aharon, 1995). The value of −26.8 ‰ observed in this peat sample is similar to those observed by a range of authors for freshwater to brackish fringe wetland environments (e.g. DeLaune, 1986; Chmura and Aharon, 1995). The common presence of secondary pyrite framboids in this unit (Fig. 5) indicates that sufficient sulphate (and Fe) was present for sulphate-reduction processes to occur, indicating a brackish, rather than freshwater, environment (e.g. Daoust et al., 1996).

4.5. Trace and major element geochemistry

Geochemical analysis focussed on cores KAM-3 and VAL-1, as these were the longest sequences recovered from each site, showed distinct (often abrupt) sedimentological changes with depth, and also contained evidence of human activity/occupation. In KAM-3, major element geochemistry primarily reflects changes in core sedimentology, with Al_2O_3, Na_2O, K_2O (not shown), and (to a lesser extent) Fe_2O_3 showing reduced concentrations in the sandier deposits between 30 and 125 cm bsl (Fig. 6). This trend is also seen for Rb, which has been widely used as an indicator of compositional changes in coastal sediments, with higher Rb values found in clay-rich sediments (e.g. Cundy et al., 2005). The heavy metals Pb, Cu and Zn show a high degree of correlation with Rb ($r>0.8$, and significant at 95% confidence, in each case), indicating that the distribution of these metals is dominantly controlled by variations in sediment composition, rather than by human (i.e. pollutant) input. Ca concentrations are relatively low throughout the core, indicating that little appreciable carbonate material is present in these sediments. In the basal dark grey/black malodorous interbedded clays and peats (3–3.5 m bsl), sulphur concentrations increase to between 0.4 and 1.6 wt.% (with no corresponding

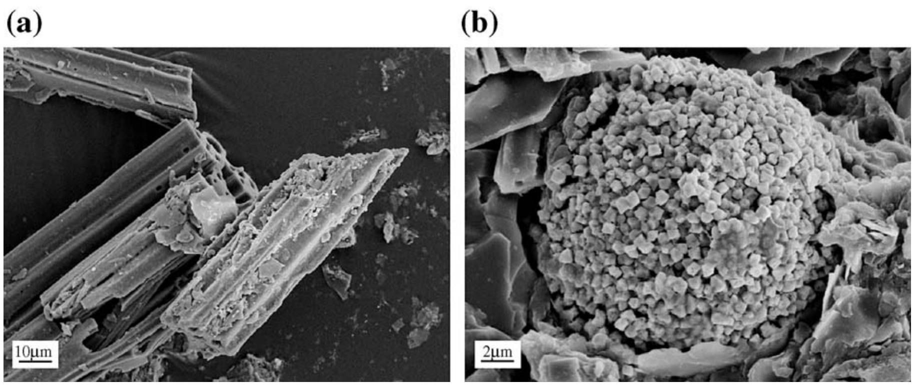

Fig. 5. Scanning electron microscope images of basal peat, Kamares Bay; (a) shows well-preserved stem material which is the dominant peat component; (b) shows example of pyrite framboid commonly found in the peat, indicating the presence of brackish to marine water. See text for discussion.

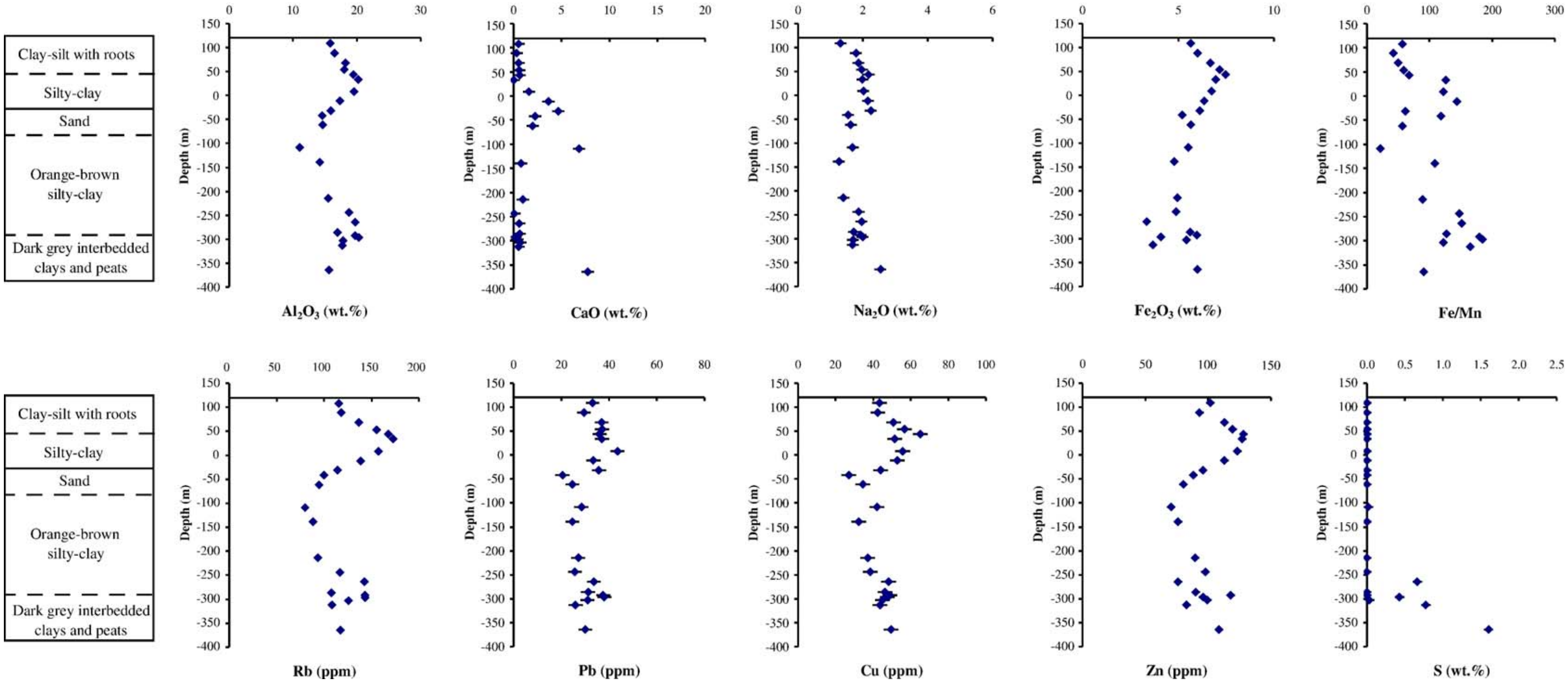

Fig. 6. Selected trace and major element data and ratios vs. depth, Kamares Bay, core KAM3. All depths are relative to contemporary sea level. Unless otherwise shown, errors on each data point are smaller than the diamond marker symbol used.

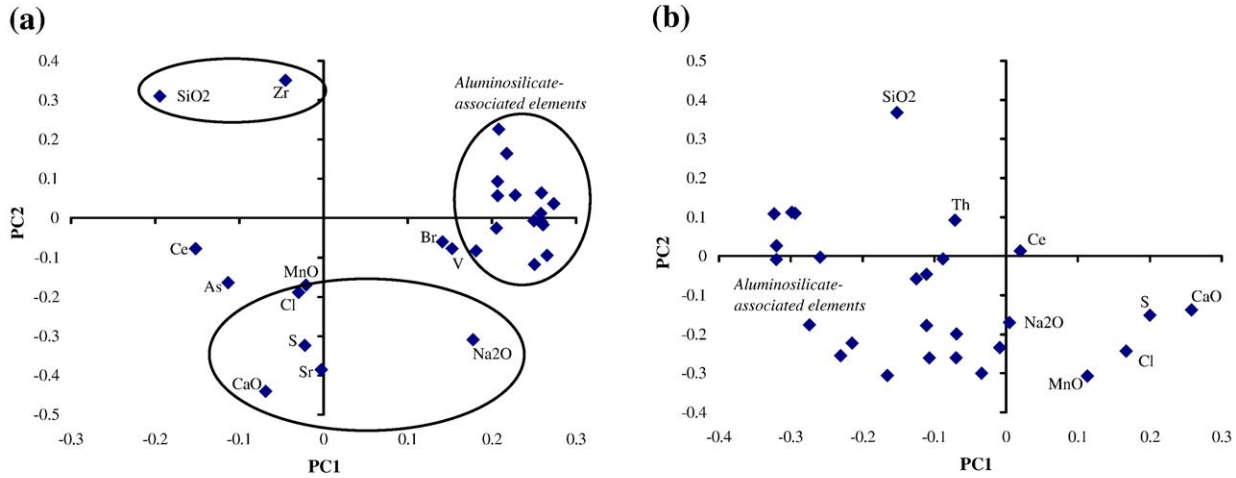

Fig. 7. Principal component loadings, plotted as Principal component 1 (PC1) loading vs. Principal Component 2 (PC2) loading for (a) Kamares Bay, core KAM3, and (b) Valtaki Bay, core VAL1. In (a), PC1 and PC2 account for 59.9% of the total variance, and in (b) 50.0% of the total variance. See text for discussion.

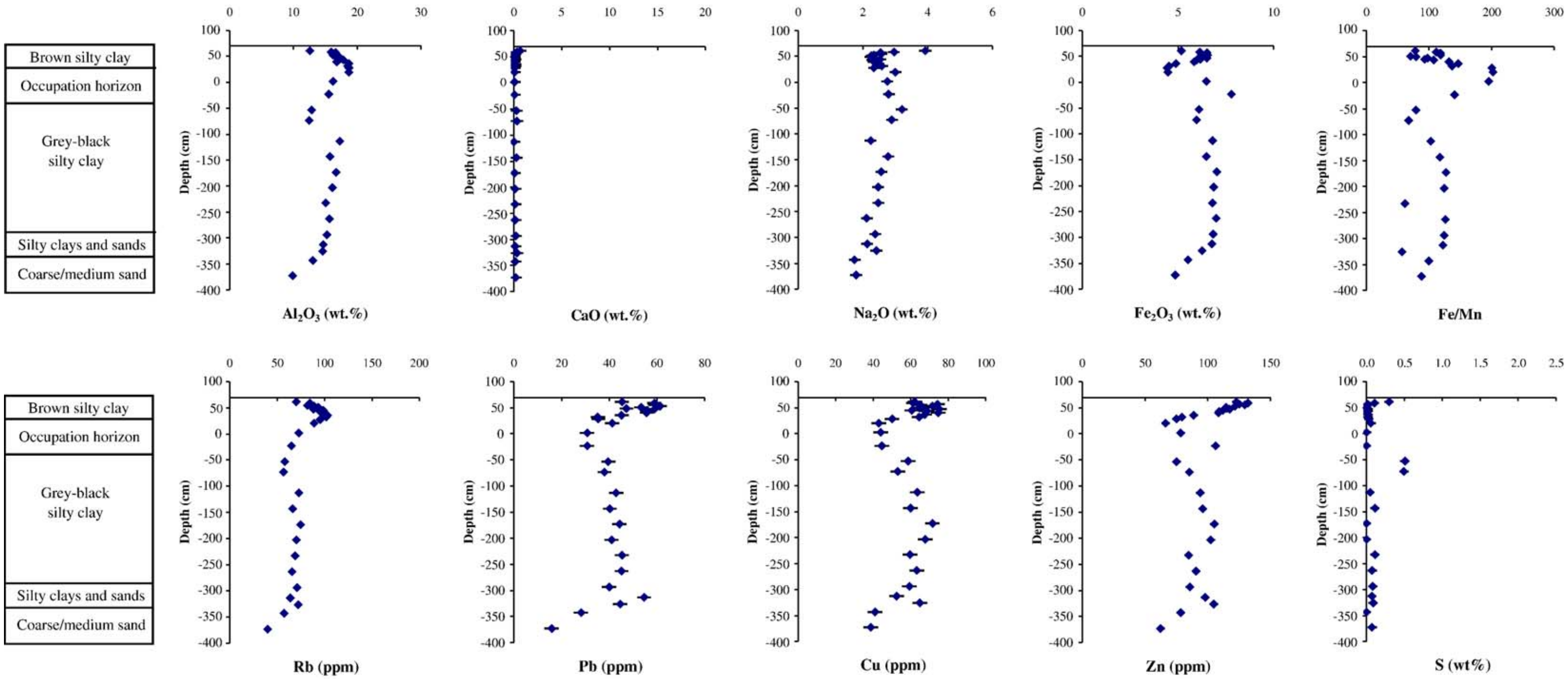

Fig. 8. Selected trace and major element data and ratios vs. depth, Valtaki Bay, core VAL1. All depths are relative to contemporary sea level. Unless otherwise shown, errors on each data point are smaller than the diamond marker symbol used.

increase in Cl), indicating enrichment of sulphur by early-diagenetic processes, due to the precipitation of insoluble metal sulphides following bacterially-mediated sulphate reduction (e.g. Pye et al., 1997). This is consistent with the observation of secondary pyrite in basal units (Section 4.4), and the dark appearance of the sediment and its strong sulphidic smell, and indicates the presence of at least brackish conditions in these deeper sediment units (e.g. Thomas and Varekamp, 1991; Daoust et al., 1996; Chague-Goff et al., 2002). The Fe/Mn ratio, which has been used as an indicator of changes in soil redox conditions in lagoonal and lake catchments (e.g. Vorren and Alm, 1999; Virkanen, 2000), is relatively erratic but does show a general decrease as sediment depth decreases, indicating a general increase in redox potential over time in the sediments and in adjacent sediment source areas. Principal component analysis (PCA) of the geochemical data supports the above observations (Fig. 7a) and allows (partial) discrimination of the elements analyzed into three main groups: (a) aluminosilicate-associated elements, including Rb, Cu, Pb, Zn, Al, K, Mg, Co; (b) a group containing Si and Zr, which are typically associated with the coarse and heavy mineral sediment fractions (e.g. Cundy et al., 2005); and (c) a group containing Ca, S, Sr, Cl and Na, which are elements noted in a number of previous studies (e.g. Chague-Goff et al., 2002) as being associated with the presence of brackish to marine conditions. The group (c) elements show the highest loadings in the basal, anoxic units.

As in core KAM-3, the major element geochemistry of core VAL-1 primarily reflects changes in sediment composition, although trends are much less distinct in this core (Fig. 8). Lower concentrations of Al_2O_3, K_2O (data not shown) and Fe_2O_3 are observed in the basal sand units (>3 m bsl), reflecting dilution of aluminosilicates (e.g. clays) by coarser, quartz-rich sands. Rb, Pb, Cu and Zn show a similar trend, although there is a notable enrichment of Pb, Cu and Zn relative to Rb at, and just below, the present-day ground surface (above 35 cm asl), possibly due to local recent human activity in the area (e.g. possible pollutant input from road traffic and a nearby car park, and sewage wastes). There is no evidence for heavy metal enrichment in the proposed occupation horizon at 45 cm bsl. Na_2O, along with Br and Cl (data not shown), is also significantly enriched at the contemporary ground surface, presumably due to evaporation of surface water in this seasonally flooded area. Ca concentrations are slightly higher than those found in KAM-3, although they are generally less than 10% (expressed as CaO), indicating limited contribution of carbonate material to the overall sediment geochemistry. CaO concentrations are however slightly elevated in the basal units and at ca. 60 cm bsl, due to the presence of small (0.5 cm diameter or less) angular carbonate clasts in the sediment matrix. Sulphur concentrations are relatively constant and uniformly lower than those observed in the basal units of KAM-3, indicating little significant sulphide formation. Fe/Mn shows little clear variability with depth, although a distinct maximum in Fe/Mn does occur at 0–30 cm asl, in a zone where sediments show clear orange-brown mottling, possibly due to fluctuations in the local water table (e.g. Cundy and Croudace, 1995). PCA gives a less clear discrimination of geochemical data than is the case in core KAM-3 (Fig. 7b), although there is some evidence for segregation of elements into the three groupings observed in KAM-3 (above).

5. Discussion

5.1. Coastal geomorphic evolution and relative sea-level history

Stratigraphic, geochemical and radiometric data from the Kamares Bay site indicate the presence of a low-energy coastal lagoon (containing brackish peats and anoxic muds, recorded in cores KAM-1 and KAM-3) from at least 3270 BP (i.e. the Late Helladic period), protected by a sand and shingle spit which was present near to the contemporary shoreline position. The presence of a beach barrier is indicated by the deeper stratigraphy of core KAM-2, where coarse sand and semi-rounded grit and gravel deposits (of similar shape and composition to the contemporary beach barrier material) occur at similar elevations to the interbedded peats and anoxic muds in the more landward cores KAM-1 and KAM-3 (Fig. 3a). In core KAM-3, a prominent brackish peat unit at 334–344 cm bsl is overlain by a dark-grey clay unit, with an S concentration of ca. 0.8 wt.%, indicating peat burial by anoxic, sulphide-rich lagoonal clays. Above the grey-black basal units present in KAM-1 and KAM-3, the concentration of sulphur declines up-core (in KAM-3), peat units disappear, the sediment becomes progressively lighter in colour and more mottled in appearance, and the Fe/Mn ratio decreases, indicating gradual infilling of the back-barrier lagoon, reduced waterlogging and development of more fresh-water/terrestrial conditions. The overall fining upward sequence observed in KAM2 indicates lowering of local energy conditions as lagoon infilling progressed. Similar late Holocene infilling of coastal embayments has been observed at a number of sites in the Aegean and the wider Mediterranean, including the nearby Plain of Elos (Kraft et al., 1977). It has been argued that such infilling is due to accelerated soil erosion from anthropogenic and/or climatic factors (e.g. Higgs, 1978). Based on the ^{14}C dates in KAM-3, the infilling at Kamares Bay was most rapid prior to the end of the Late Roman period. Notably, this infilling of the lagoon and development of more terrestrial conditions indicates that the net vertical sediment accumulation rate at the site (1.3 mm/yr between ca. 1500 BC and the present day) must exceed the combined rate of local sea-level rise and any decrease in elevation of the sediment surface due to compaction effects (see below). The presence of periodic coarser sediment layers in KAM-1 and KAM-3 suggest that changes in stream activity or barrier overwash events have occasionally produced higher energy sedimentation. The lack of stratigraphically-continuous coarse sediment units which can be correlated between individual cores indicate that localised stream/alluvial changes are more likely to be responsible for these episodes of higher energy sedimentation.

The coastal stratigraphy at Valtaki is less informative, although a general fining upwards sequence from coarse sand at the base to silt and clay-rich units at shallower depths is observed in VAL-1, which is consistent with lowering of local energy conditions and infilling of a back-barrier area. The interbedded basal peats and anoxic clays observed in Kamares Bay are not present in the VAL-1 sequence however, possibly due to the site's proximity to the coastal barrier (as in KAM-2 above). In core VAL-2, from the northeastern end of the bay, the stratigraphy is dominated by massive, well-sorted sands until very near to the contemporary sediment surface, and there is no stratigraphic (or local archaeological) evidence for occupation. This indicates significant spatial variation in palaeoenvironment across the bay, with a spit-protected, low-lying, occupied (at least in Late Roman times) area in the southwest of the bay, with possibly an open coastal or dune-dominated area in the northeast of the bay.

Both sites show evidence for past human activity. In core KAM-3, a unit containing brick fragments and large fragments of charcoal dates to ca. 450 AD (Late Roman). An apparent Late Roman occupation horizon is also found at, and slightly below, contemporary sea level in VAL-1. The stratigraphic and archaeological evidence point towards much more intensive Late Roman use of the Valtaki site than Kamares Bay. Despite this, however, there is no evidence for any pollutant metal enrichment in the occupation horizon at Valtaki, or indeed in the macro-charcoal layer at Kamares Bay: Pb, Cu and Zn all show good correlations with the sediment compositional indicator Rb, indicating that the distribution of these metals is dominantly controlled by mineralogical variations, rather than pollutant input. Hence, there is no evidence for significant local metal-working activity. While isolated brick/tile fragments are present at 182 cm bsl in KAM-3, there is little clear stratigraphic evidence for significant pre-Roman activity at either the Kamares or the Valtaki sites.

The presence of an apparently brackish peat unit, overlain by anoxic (lagoonal) muds, at 3.4 m bsl in the Kamares Bay site is significant. The microtidal regime in the Mediterranean means that such brackish marsh peats have a relatively close relationship with local relative sea level, and the presence of this buried peat indicates a rise in relative sea level of ca. 3.4 m since 1630–1440 BC (the calibrated age of the peat), i.e. 0.8–1 mm/yr. Local archaeological data also indicate a relative sea-level rise in the study area during the late Holocene, with slightly submerged Late Roman archaeological remains present at Valtaki. There is also evidence of landward migration of the barrier at Valtaki, with Late Roman walls partly-buried by the contemporary dune system, and eroding beach rocks present in the subtidal beach face (Fig. 2b). The proposed occupation horizon found in core VAL-1 also clearly extends below contemporary high water sea level. The 0.8–1 mm/yr sea-level rise calculated using the buried peat at Kamares Bay is clearly an estimate, as the lack of preserved microfossils mean that a detailed sea-level index point cannot be established. The estimate is, however, corroborated by published sea-level data for the area. Flemming (1968) isolated three coastal archaeological sites in the immediate vicinity of Gythio, dated at 1000–1500 yr old, which were submerged by 1.0–2.5 m, and in a later study Flemming and Webb (1986) calculate a tectonic depression rate in the Gythio area of 1 m per 1000 yr (caused by a general regional tectonic depression across the margins of the Peloponnese). In stratigraphic studies of the nearby Plain of Elos, Kraft et al. (1977) date a backswamp peat at −6 m to ca. 4000 BC, indicating a local relative sea-level rise of 1 mm/yr over the late Holocene at this site, while a combined eustatic and glacio-hydrostatic sea-level model produced for the Aegean by Lambeck in 1996 (see also Lambeck and Purcell, 2005) estimates a ca. 1.5 m sea-level rise in the southern Peloponnese over the last 2000 yr.

5.2. Evidence of local and regional seismic activity and tsunami inundation

The similarity between the 0.8–1 mm/y rate of sea-level rise determined at the Kamares Bay site, and that determined in Lambeck's (1996) regional eustatic and glacio-hydrostatic sea-level model, indicates that (over the late Holocene timescale studied here) there have been no major vertical displacements in coastal elevation caused by local tectonic activity (i.e. movements on local fault strands). It is also interesting to note that the stratigraphy at Kamares Bay contains no discrete and continuous sand layers which may be associated with rapid marine inundation from tsunami (or indeed storm) flooding, or geochemical evidence for such a phenomenon, in spite of the presence of the area in a seismically active zone known to be subject to periodic tsunami (see Section 2). The data indicate that those tsunami events which have been recorded in earthquake and tsunami catalogues were of insufficient magnitude to overwash the protective spit present at the shoreline and/or leave a discernible sedimentary signature. The burning of local vegetation, and possible burning of human artefacts, indicated by the charcoal and burnt ceramic-rich occupation horizon at 38–47 cm asl in core KAM-3, arguably could be related to earthquake destruction. The calibrated ^{14}C age of the charcoal in this unit however, postdates the 365 AD Cretan earthquake, the only major event recorded in this area in the Late Roman/Early Byzantine era. It is therefore likely that this charcoal layer is related to other causes, such as accidental or deliberate vegetation burning for land clearance. Notably, the upper part of the calibrated ^{14}C age range for the peat at 3.4 m bsl in the KAM-3 core covers the published age range for the so-called Minoan tsunami, proposed as being associated with explosive eruption of the Thera (Santorini) volcano in ca. 1627 BC (Minoura et al., 2000). This volcanic eruption is suggested to have resulted in an eastern Mediterranean-wide tsunami, with wave heights in excess of 5 m along the western Turkish and Cretan coasts (Minoura et al., 2000, although see critical review of evidence by Dominey-Howes, 2004). There is no evidence in the sequences cored at Kamares Bay of either any significant tephra deposition associated with the volcanic eruption, or discrete marine-derived sand layers which may indicate wave inundation from the tsunami. Given the error range on the calibrated radiocarbon age, however, any deposits associated with the 1627 BC Thera eruption (if present) may be found in deeper units than those cored here.

5.3. Use of geochemical studies in the reconstruction of palaeo-sea levels and coastal evolution

Wilson et al. (2005) note the potential usefulness of geochemical (specifically $\delta^{13}C$ and C/N) analysis of organic matter in the reconstruction of sea-level histories. The data presented here supports earlier work (e.g. Thomas and Varekamp, 1991; Goff and Chague-Goff, 1999; Chague-Goff et al., 2002) that indicates that bulk trace and major element sediment geochemistry may also be a useful tool in coastal palaeoenvironmental reconstruction, in discriminating brackish/marine from freshwater sedimentary units, in the examination of changes in soil/sediment redox potential over time, and as a proxy for grain size/sediment composition. Sediment geochemistry may also provide a useful method of dating or of correlating coastal sediment units (e.g. Cundy and Croudace, 1995; Gehrels et al., 2005). Given the much greater accuracy that can be achieved using microfossils to determine sea-level index points however, as with $\delta^{13}C$ and C/N studies, the use of bulk sediment geochemistry in examining sea-level histories is likely to be most useful in sediments (such as those discussed here) where the initial concentrations of microorganisms are low, or where the preservation of microfossils is poor.

6. Conclusions

The coastal sediment sequences at Kamares (Kato Vathi) Bay show clear stratigraphic and geochemical evidence of the presence in Late Helladic times of a barrier-protected coastal lagoonal environment, which has gradually infilled over the last ca. 3500 yr. The coastal stratigraphy at Valtaki Bay is less informative, although a general fining upwards sequence (which underlies an apparent Late Roman occupation horizon) in the southwest of the bay indicates the gradual infilling of a back-barrier wetland or lagoon, present in pre-Roman times. In contrast, the stratigraphy in the northeastern part of Valtaki Bay is dominated by massive, well-sorted sand units until very near to the contemporary sediment surface, indicating the presence (until recently) of a more open coastal or dune-dominated area here. An apparent brackish wetland peat deposit at 3.4 m bsl (overlain by anoxic lagoonal clays) at Kamares Bay shows a calibrated radiocarbon age of 1640–1440 BC, indicating a relative sea-level rise of 0.8–1 mm/yr in this area over the past 3500 yr, in good agreement with previous archaeological and sea-level modelling studies. Archaeological remains, an apparent occupation horizon within the cored sediment sequence at Valtaki, and dated macro-charcoal from the Kamares Bay site indicate Late Roman occupation of the area, although there is no sedimentary evidence of significant pre-Roman activity at the study sites. There is no evidence, based on the stratigraphic, microfossil or geochemical record, of sudden marine flooding events related to local or regional seismic activity. More generally, the data (particularly at Kamares Bay) highlight the utility of combining geochemical and stratigraphic studies in the reconstruction of coastal evolution and the study of palaeo-sea level using coastal sediment sequences, particularly in sediments (such as those present here) where microfossils commonly used as sea-level indicators (e.g. foraminifera and diatoms) are poorly preserved.

References

Appleby, P.G., Oldfield, F., 1992. Applications of ^{210}Pb to sedimentation studies, In: Harmon, R.S., Ivanovich, M. (Eds.), Uranium-series disequilibrium. Applications to earth, marine and environmental sciences, 2nd Edition. Oxford Science, Oxford.

Chague-Goff, C., Dawson, S., Goff, J.R., Zachariasen, J., Berryman, K.R., Garnett, D.L., Waldron, H.M., Mildenhall, D.C., 2002. A tsunami (c. 6300 years BP) and other Holocene environmental changes, northern Hawke's Bay, New Zealand. Sediment. Geol. 150, 89–102.

Chmura, G.L., Aharon, P., 1995. Stable carbon isotope signatures of sedimentary carbon in coastal wetlands as indicators of salinity regime. J. Coast. Res. 11, 124–135.

Cundy, A.B., 2005. Recent rapid sea-level change in the eastern Mediterranean and the coastal sedimentary record. Z. Geomorphol. 29–35 Suppl.-Vol. 137.

Cundy, A.B., Croudace, I.W., 1995. Sedimentary and geochemical variations in a salt marsh/mud flat environment from the mesotidal Hamble estuary, southern England. Mar. Chem. 51, 115–132.

Cundy, A.B., Croudace, I.W., 1996. Sediment accretion and recent sea level rise in the Solent, southern England: inferences from radiometric and geochemical studies. Estuar. Coast. Shelf Sci. 43, 449–467.

Cundy, A.B., Kortekaas, S., Dewez, T., Stewar, I.S., Collins, P.E.F., Croudace, I.W., Maroukian, H., Papanastassiou, D., Gaki-Papanastassiou, P., Pavlopoulos, K., Dawson, A., 2000. Coastal wetlands as recorders of earthquake subsidence in the Aegean: a case study of the 1894 Gulf of Atalanti earthquakes, central Greece. Mar. Geol. 170, 3–26.

Cundy, A.B., Long, A.J., Hill, C.T., Spencer, C., Croudace, I.W., 2002. Sedimentary response of Pagham Harbour, southern England to barrier breaching in AD 1910. Geomorphology 46, 163–176.

Cundy, A.B., Croudace, I.W., Cearreta, A., Irabien, M.J., 2003. Reconstructing historical trends in metal input in heavily-disturbed, contaminated estuaries: studies from Bilbao, Southampton Water and Sicily. Appl. Geochem. 18, 311–325.

Cundy, A.B., Hopkinson, L., Lafite, R., Spencer, K., Taylor, J.A., Ouddane, B., Heppell, C.M., Carey, P.J., Charman, R., Shell, D., Ullyott, S., 2005. Heavy metal distribution and accumulation in two Spartina sp.-dominated macrotidal salt marshes from the Seine estuary (France) and the Medway estuary (U.K.). Appl. Geochem. 20, 1195–1208.

Daoust, R.J., Morre, T.R., Chmura, G.L., Magenheimer, J.F., 1996. Chemical evidence of environmental changes and anthropogenic influences in a Bay of Fundy salt marsh. J. Coast. Res. 12, 520–533.

DeLaune, R.D., 1986. The use of δ^{13}C signature of C-3 and C-4 plants in determining past depositional environments in rapidly accreting marshes of the Mississippi river deltaic plain, Louisiana, USA. Chem. Geol. 59, 315–320.

Devoy, R.J.N., Delaney, C., Carter, R.W.G., Jennings, S.C., 1996. Coastal stratigraphies as indicators of environmental changes upon European Atlantic coasts in the Late Holocene. J. Coast. Res. 12, 564–588.

Dominey-Howes, D., 2004. A re-analysis of the Late Bronze Age eruption and tsunami of Santorini, Greece, and the implications for the volcano-tsunami hazard. J. Volcanol. Geotherm. Res. 130, 107–132.

Flemming, N.C., 1968. Holocene earth movements and eustatic sea-level change in the Peloponnese. Nature 217, 1031–1032.

Flemming, N.C., Webb, C.O., 1986. Tectonic and eustatic coastal changes during the last 10,000 years derived from archaeological data. Z. Geomorphol. 1–29 Suppl. Vol. 62.

Gaki-Papanastassiou, K., Papanastassiou, D., Maroukian, H., 2006a. Recent uplift rates at Perachora peninsula, east Gulf of Corinth, Greece, based on geomorphological-archaeological evidence and radiocarbon dates. Hell. J. Geol. 42, 78–96.

Gaki-Papanastassiou, K., Maroukian, H., Tsartsidou, G., 2006b. Late Quaternary morphological changes along the western shores of the Lakonic gulf (Peloponnesus, Greece) based on geomorphological and archaeological data. Hell. J. Geol. 42, 133–145.

Gehrels, W.R., 2002. Intertidal foraminifera as palaeoenvironmental indicators. In: Haslett, S.K. (Ed.), Quaternary Environmental Micropalaeontology. Arnold, London, pp. 91–114.

Gehrels, W.R., Kirby, J.R., Prokoph, A., Newnham, R.M., Achterberg, E.P., Evans, H., Black, S., Scott, D.B., 2005. Onset of recent rapid sea-level rise in the western Atlantic Ocean. Quat. Sci. Rev. 24, 2083–2100.

Goff, J.R., Chague-Goff, C., 1999. A Late Holocene record of environmental changes from coastal wetlands: Abel Tasman National Park, New Zealand. Quat. Int. 56, 39–51.

Griffiths, H.I., Holmes, J.A., 2000. Non-marine ostracods and Quaternary palaeoenvironments. Technical Guide 8. Quaternary Research Association, London. 188 pp.

Hamilton, S., Shennan, I., 2005. Late Holocene great earthquakes and relative sea-level change at Kenai, southern Alaska. J. Quat. Sci. 20, 95–111.

Higgs, E., 1978. Environmental changes in northern Greece. In: Brice, W.C. (Ed.), The environmental history of the Near to Middle East since the last ice age. Academic Press, London, pp. 41–49.

Islam, M.S., Tooley, M.J., 1999. Coastal and sea-level changes during the Holocene in Bangladesh. Quat. Int. 55, 61–75.

Kershaw, S., Guo, L., Braga, J.C., 2005. A Holocene coral-algal reef at Mavra Litharia, Gulf of Corinth, Greece: structure, history and applications in relative sea-level change. Mar. Geol. 215, 171–192.

Kraft, J.C., Aschenbrenner, S.E., Rapp Jr., G., 1977. Paleogeographic reconstructions of coastal Aegean archaeological sites. Science 195, 941–947.

Laborel, J., Laborel-Deguen, F., 1994. Biological indicators of relative sea-level variations and of coseismic displacements in the Mediterranean region. J. Coast. Res. 10, 395–415.

Lambeck, K., 1996. Sea-level change and shoreline evolution in Aegean Greece since Upper Palaeolithic time. Antiquity 70, 588–611.

Lambeck, K., Purcell, A., 2005. Sea-level change in the Mediterranean Sea since the LGM: model predictions for tectonically stable areas. Quat. Sci. Rev. 24, 1969–1988.

Long, A.J., Shennan, I., 1994. Sea-level changes in Washington and Oregon and the "Earthquake Deformation Cycle". J. Coast. Res. 10, 825–838.

Maroukian, H., Gaki-Papanastassiou, P., Papanastassiou, D., 1994. Coastal changes in Corinthia, Greece. In: Swiny, S., Hohlfelder, R.L., Swiny, H.W. (Eds.), Proceedings of the second international symposium "Cities on the Sea", Nicosia, Cyprus. Cyprus American Archaeological Research Institute Monograph Series, vol. 1, No. 24. Scholars Press, Atlanta, pp. 217–226. October 18–22.

Mackie, E.A.V., Leng, M.J., Lloyd, J.M., Arrowsmith, C., 2005. Bulk organic δ^{13}C and C/N ratios as palaeosalinity indicators within a Scottish isolation basin. J. Quat. Sci. 20, 303–312.

Minoura, K., Imamura, F., Kuran, U., Nakamura, T., Papadopoulos, G.A., Takahashi, T., Yalciner, A.C., 2000. Discovery of Minoan tsunami deposits. Geology 28, 59–62.

Nelson, A.R., Shennan, I., Long, A.J., 1996. Identifying coseismic subsidence in tidal-wetland stratigraphical sequences at the Cascadia subduction zone of western North America. J. Geophys. Res. 101 (B3), 6115–6135.

Panagopoulou, E., Karkanas, P., Tsartsidou, G., Harvati, K., Kotabopoulou, E., Dinou, M., 2002. Late Pleistocene archaeological and fossil human evidence from Lakonis cave, southern Greece. J. Field Archaeol. 29, 323–249.

Papazachos, B.C., Papazachou, C.B., 1997. The earthquakes of Greece, vol. 304. Ziti Publ, Thessaloniki, p. 1997.

Pirazzoli, P.A., 2005. Marine erosion features and bioconstructions as indicators of tectonic movements, with special attention to the eastern Mediterranean area. Z. Geomorphol. 71–77 Suppl. Vol. 137.

Pye, K., Coleman, M.L., Duan, W.M., 1997. Microbial activity and diagenesis in salt marsh sediments, North Norfolk, England. In: Jickells, T., Rae, J.E. (Eds.), Biogeochemistry of Intertidal Sediments. Cambridge University Press, pp. 119–151.

Reimer, P.J., Baillie, M.G.L., Bard, E., Bayliss, A., Beck, J.W., Bertrand, C.J.H., Blackwell, P.G., Buck, C.E., Burr, G.S., Cutler, K.B., Damon, P.E., Edwards, R.L., Fairbanks, R.G., Friedrich, M., Guilderson, T.P., Hogg, A.G., Hughen, K.A., Kromer, B., McCormac, F.G., Manning, S.W., Ramsey, C.B., Reimer, R.W., Remmele, S., Southon, J.R., Stuiver, M., Talamo, S., Taylor, F.W., van der Plicht, J., Weyhenmeyer, C.E., 2004. IntCal04 terrestrial radiocarbon age calibration, 26–0 ka BP. Radiocarbon 46, 1029–1058.

Ritchie, J.C., McHenry, J.R., Gill, A.C., 1990. Application of radioactive fallout Cs-137 for measuring soil erosion and sediment accumulation rates and patterns: a review. J. Environ. Qual. 19, 215–233.

Stiros, S.C., Laborel, J., Laborel-Deguen, F., Papageorgiou, S., Evin, J., Pirazzoli, P.A., 2000. Seismic coastal uplift in a region of subsidence: Holocene raised shorelines of Samos Island, Aegean Sea, Greece. Mar. Geol. 170, 41–58.

Stuiver, M., Reimer, P.J., 1993. Extended ^{14}C database and revised CALIB radiocarbon calibration program. Radiocarbon 35, 215–230.

Thomas, E., Varekamp, J.C., 1991. Palaeo-environmental analyses of marsh sequences (Clinton, Connecticut): evidence for punctuated rise in sea level during the latest Holocene. J. Coast. Res. 11, 125–158.

Virkanen, J., 2000. The effects of natural environmental changes on sedimentation in Lake Kuttanen, a small closed lake in Finnish Lapland. Holocene 10, 377–386.

Vorren, K.D., Alm, T., 1999. Late Weichselian and Holocene environments of lake Endletvatn, Andoya, northern Norway: as evidenced primarily by chemostratigraphic data. Boreas 28, 505–520.

Wilson, G.P., Lamb, A.L., Leng, M.J., Gonzalez, S., Huddart, D., 2005. $\delta^{13}C$ and C/N as potential coastal palaeoenvironmental indicators in the Mersey Estuary, UK. Quat. Sci. Rev. 24, 2015–2029.